Chinese Journal of
POLYMER SCIENCE

RESEARCH ARTICLE

https://doi.org/10.1007/s10118-026-3845-9
Chinese J. Polym. Sci.

Photoinduced Cationic Reversible Addition–Fragmentation Chain Transfer 3D Printing Using 'Green' Chain Transfer Agent

Ying Zhu[a,†], Wen-Hui Li[a,†], Shu-Han Ling[a], Fukuda Shinichiroh[b], Zhi-Hua He[b], Jia-Jia Li[a*], and Jian Zhu[a,c*]

[a] *State and Local Joint Engineering Laboratory for Novel Functional Polymeric Materials, Jiangsu Key Laboratory of Advanced Functional Polymer Design and Application, Department of Polymer Science and Engineering, College of Chemistry, Chemical Engineering and Materials Science, Soochow University, Suzhou 215123, China*
[b] *Taiyo Ink Suzhou Co. Ltd., Suzhou 215129, China*
[c] *Analysis and Testing Center, Soochow University, Suzhou 215123, China*

Electronic Supplementary Information

Abstract The integration of reversible deactivation polymerization mechanisms into three-dimensional (3D) printing offers unique opportunities to construct living polymer networks with tunable properties and post-fabrication modification capabilities. However, conventional reversible addition–fragmentation chain transfer (RAFT) agents typically exhibit strong visible-light absorption, resulting in undesirable coloration that limits their use in optical and transparent applications. Herein, we report a photoinduced radical-promoted cationic RAFT (RPC-RAFT) polymerization system employing a colorless "green" chain transfer agent (CTA) for digital light processing (DLP) 3D printing. Controlled polymerization of various vinyl ethers was achieved within minutes under 405 nm irradiation, affording polymers with predictable molecular weights (M_n=5000–15800 g·mol^{-1}) and relatively narrow molecular weight distributions. Moreover, photocurable resins suitable for DLP printing were developed, enabling fabrication of complex architectures The resulting objects exhibited excellent shape fidelity and tunable mechanical properties, establishing a practical strategy for colorless and transparent living 3D printing and expands the scope of cationic RAFT polymerization for advanced additive manufacturing applications.

Keywords 3D printing; Photopolymerization; Cationic polymerization; Reversible addition–fragmentation chain transfer polymerization

Citation: Zhu, Y.; Li, W. H.; Ling, S. H.; Shinichiroh, F.; He, Z. H.; Li, J. J.; Zhu, J. Photoinduced cationic reversible addition–fragmentation chain transfer 3D printing using 'green' chain transfer agent. *Chinese J. Polym. Sci.* https://doi.org/10.1007/s10118-026-3845-9

INTRODUCTION

Photopolymerization-based three-dimensional (3D) printing technologies have revolutionized modern manufacturing by enabling rapid fabrication of complex architectures with high resolution and precise spatiotemporal control. These techniques have found widespread application in microfluidics, biomedical devices, soft robotics, and tissue engineering.[1–5] Recently, the integration of reversible deactivation radical polymerization (RDRP),[6–8] such as reversible addition-fragmentation chain transfer (RAFT) polymerization,[9–12] nitroxide mediated polymerization (NMP),[13,14] and atom transfer radical polymerization (ATRP),[15] into 3D printing has emerged as a powerful strategy for constructing "living" polymer networks.[16,17] Such systems not only enable precise control over the network structure and the resulting macroscopic and microscopic properties but also provide opportunities for post-printing modifications, thereby expanding the scope of smart and customizable materials.

In addition to RDRP-based approaches, cationic RAFT polymerization,[18–20] originally developed by Kamigaito *et al*., has emerged as an effective strategy for controlling the polymerization of cationically polymerizable monomers. Recently, our group successfully integrated radical-promoted cationic (RPC)-RAFT polymerization into commercial digital light-processing (DLP) 3D printing, demonstrating the feasibility of fabricating living 3D objects.[21,22] However, conventional RAFT agents, such as dithiocarbamates and trithiocarbonates, exhibit strong absorption in the visible region and impart undesirable coloration to printed objects. This inherent limitation restricts their application in fields that require high optical transparency, such as optical components and transparent microfluidic devices. To address this challenge, Fors *et al*. reported a readily accessible "green" chain transfer agent (CTA) that can be synthesized on a 50 g scale in 83% yield under aqueous, room-temperature conditions, consistent with the principles of green chemistry.[23] Importantly, CTA was obtained as a white crystalline solid, allowing purification by recrystallization rather than solvent-intensive column chro-

* Corresponding authors, E-mail: chemjjli@suda.edu.cn (J.J.L.)
E-mail: chemzhujian@suda.edu.cn (J.Z.)
† These authors contributed equally to this work.
Received July 28, 2026; Accepted August 13, 2026; Published online November 12, 2026

© Chinese Chemical Society
Institute of Chemistry, Chinese Academy of Sciences

matography. Although photoinduced cationic RAFT polymerization mediated by this CTA was demonstrated using 2,4,6-tris(4-methoxyphenyl)pyrylium tetrafluoroborate (PMP) as a photocatalyst, the polymerization proceeded relatively slowly, requiring 19.5 h to achieve 81% monomer conversion. Such sluggish kinetics are incompatible with photopolymerization-based 3D printing, in which rapid curing is essential. Our previous studies demonstrated that a combination of diphenyliodonium hexafluorophosphate (DPI) and diphenyl(2,4,6-trimethylbenzoyl)phosphine oxide (TPO) can significantly accelerate photoinduced cationic RAFT polymerization through an RPC-RAFT mechanism (Fig. 1a).[21] Building upon this strategy, herein we report a DLP 3D printing system based on photoinduced RPC-RAFT polymerization employing the "green" CTA (Fig. 1b). This approach enables rapid fabrication of colorless, highly transparent living polymer networks while maintaining the advantages of controlled cationic polymerization.

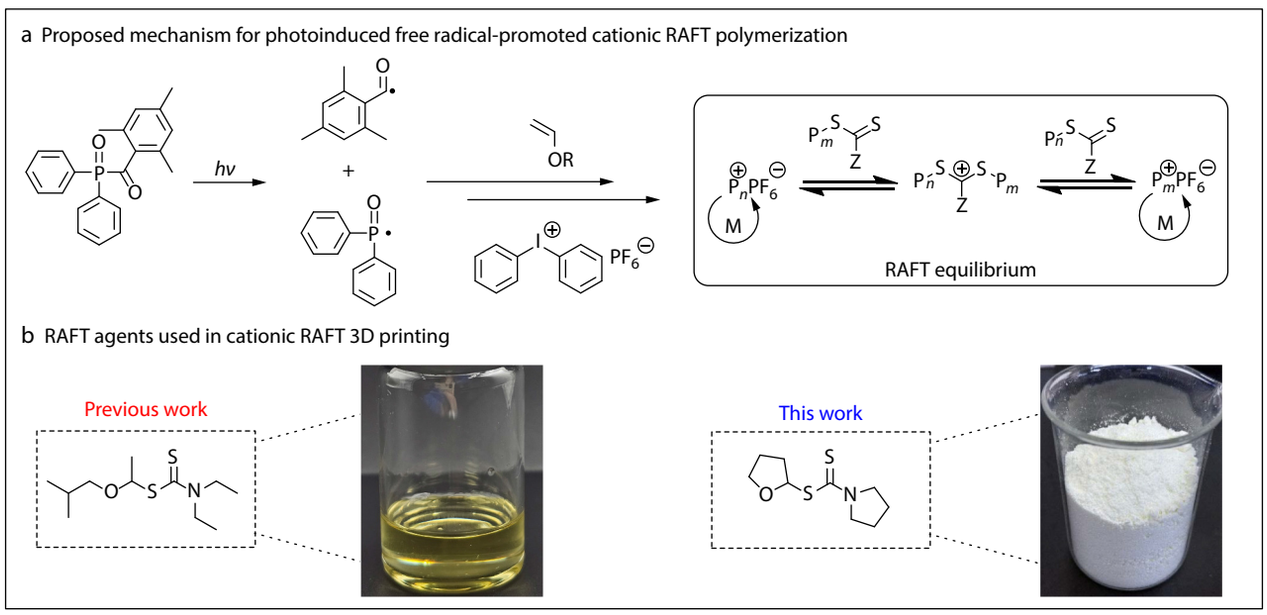


Fig. 1 (a) Proposed mechanism for photoinduced free radical-promoted cationic RAFT polymerization; (b) RAFT agents used in cationic RAFT 3D printing.

EXPERIMENTAL

Procedure For Photopolymerization of IBVE

The monomers were dried over CaH_2 for at least 12 h, distilled under nitrogen, subjected to three freeze–pump–thaw cycles, and stored in a glovebox. In a typical experiment, IBVE (386.5 mg, 3.86 mmol), CTA (8.37 mg, 0.0386 mmol), TPO (0.82 mg, 0.0019 mmol), DPI (0.67 mg, 0.0019 mmol) and DCM (0.5 mL) were added to a 4 mL Teflon vial ($[IBVE]_0$:$[CTA]_0$:$[TPO]_0$:$[DPI]_0$ = 100:1:0.05:0.05). The mixture was irradiated with a 405 nm LED (1.1 mW·cm^{-2}) at 25 °C under stirring for the desired time. The reaction was quenched by dilution with THF and addition of trace methanol. The monomer conversion was determined gravimetrically.

3D Printing Procedure

A resin mixture (about 17 mL) containing DDE, DHF, CTA, TPO and DPI with a molar ratio of $[DDE]_0$:$[DHF]_0$:$[CTA]_0$:$[TPO]_0$:$[DPI]_0$ = 50:50:5:0.1:0.1 was poured into the sink of the DLP 3D printer. The mold.stl file was then imported into the printer. The printing parameters were set as follow: exposure time per layer: 50 s; target per layer thickness: 0.1 mm; 1 bottom layer and 55 s exposure time for bottom layer; 1 for anti-alias; 5 mm Z lift height; 2 mm·s^{-1} Z lift speed; 2 mm·s^{-1} Z retract step speed. Subsequently, the printing process was initiated. The printed objects were washed with ethyl acetate.

RESULTS AND DISCUSSION

We first investigated the model polymerization of isobutyl vinyl ether (IBVE) under 405 nm irradiation in the presence of TPO and DPI. As summarized in Table 1, entries 1–4, increasing the concentrations of DPI and TPO enabled high monomer conversions to be achieved within minutes while maintaining good control over molecular weight and relatively narrow molecular weight distributions (MWDs). Furthermore, the number-average molecular weight (M_n) was readily tuned by varying the initial molar ratio of IBVE to CTA (Table 1, entries 5 and 6). When higher degrees of polymerization were targeted, broader MWDs were observed (Table 1, entries 7 and 8), likely due to irreversible chain transfer or termination reactions. Control experiments confirmed the essential role of each component. In the absence of CTA, the resulting polymer exhibited a broad MWD ($Đ$=1.97, Table 1, entry 9), indicating the loss of degenerative chain transfer control. Moreover, no polymerization occurred without light irradiation or DPI (Table 1, entries 10 and 11), demonstrating that photoactivation is indispensable for generating initiating cationic species. A lower monomer conversion was observed in the absence of TPO, suggesting a lower decomposition efficiency of DPI (Table 1, entry 12).

The polymerization kinetics were subsequently investigated at room temperature using a $[IBVE]_0$:$[CTA]_0$:$[TPO]_0$:$[DPI]_0$ molar ratio of 100:1:0.05:0.05. As shown in Fig. 2(a), a linear re-

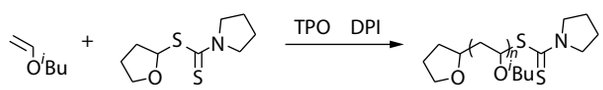
https://doi.org/10.1007/s10118-026-3845-9

lationship between $\ln([M]_0/[M])$ and the reaction time was observed, indicating pseudo-first-order kinetics and a constant concentration of propagating species throughout the polymerization. The experimentally determined molecular weights increased linearly with monomer conversion, whereas the MWDs remained relatively narrow over the entire conversion range (Fig. 2b). In addition, size exclusion chromatography (SEC) traces shifted progressively toward higher molecular weights while retaining unimodal and symmetric distributions (Fig. S3 in the electronic supplementary information, ESI), consistent with the characteristics of a living polymerization process.

The monomer scope was evaluated using a variety of vinyl ethers, including ethyl vinyl ether (EVE), propyl vinyl ether (PVE), butyl vinyl ether (BVE), 2,3-dihydrofuran (DHF), and cyclohexyl vinyl ether (CHVE). As summarized in Table 2, controlled molecular weights and relatively narrow MWDs were obtained for most of the monomers (entries 1–3). In contrast, poly(DHF) and poly(CHVE) exhibited broader MWDs (entries 4–5), probably because of the increased steric hindrance associated with the cyclic monomer structures.[24]

To establish a practical 3D printing platform, diethylene glycol divinyl ether (DDE) was incorporated as a crosslinker into a photocurable resin containing DHF, CTA, TPO, and DPI. The molar ratio of DDE, DHF, CTA, TPO, and DPI was fixed at 50:50:1:0.1:0.1. The printing performance was systematically evaluated by varying the exposure time and the target layer thickness. As summarized in Fig. 3 and Table S1 (in ESI), well-defined three-dimensional objects were successfully fabricated at maximum printing speeds of 4.44, 2.29, and 1.08 $cm \cdot h^{-1}$ for layer thicknesses of 200, 100, and 50 μm, respectively. Using the optimized formulation and printing parameters, a range of complex structures, including the character "fortune", Mayan pyramid, and Roman column, were successfully fabricated (Fig. 4). The printed objects exhibited excellent shape fidelity and a smooth surface morphology, highlighting the excellent printability of the resin system. Notably, all printed objects were colorless and highly transparent because the "green" CTA exhibits negligible absorption in the visible region, thereby eliminating the coloration commonly associated with conventional RAFT agents. These results collectively demonstrate the feasibility of photoinduced RPC-

Table 1 Polymerization of IBVE in DCM under various conditions at 25 °C under a 405 nm LED light (1.1 $mW \cdot cm^{-2}$), V_{IBVE}=0.5 mL, V_{DCM}=0.5 mL.



Entry	$[IBVE]_0:[CTA]_0:[TPO]_0:[DPI]_0$	Time (min)	Conv. (%)	$M_{n,th}$ [a]	$M_{n,SEC}$ [b]	$Đ$
1	100:1:0.01:0.01	120.0	77	7900	5000	1.33
2	100:1:0.03:0.03	60.0	91	9300	7500	1.30
3	100:1:0.05:0.05	7.0	96	9800	9300	1.22
4	100:1:0.1:0.1	3.5	98	10000	8300	1.28
5	50:1:0.05:0.05	5.0	>99	5200	5100	1.18
6	200:1:0.05:0.05	20.0	96	19400	15800	1.31
7	300:1:0.05:0.05	55.0	99	30000	18800	1.45
8	500:1:0.05:0.05	90.0	97	48800	19100	1.67
9	100:0:0.05:0.05	3.5	>99	–	16100	1.97
10	100:1:0.05:0	10.0	–	–	–	–
11 [c]	100:1:0.05:0.05	24.0 h	–	–	–	–
12	100:1:0:0.05	10.0	28	3000	3400	1.43

[a] Calculated based on conversion ($M_{n,th}$ = $[IBVE]_0/[CTA]_0 \times M_{IBVE}$ ×conversion + M_{CTA}); [b] Determined by tetrahydrofuran (THF) SEC using polystyrene (PS) calibration (note: these values are relative molecular weights for poly(vinyl ether)s); [c] Polymerization in the dark.

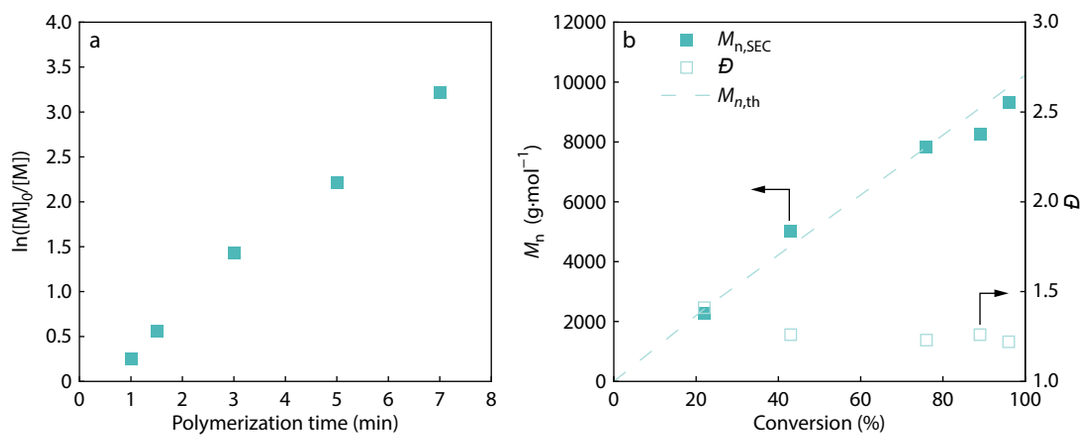
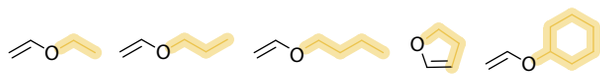


Fig. 2 Polymerization of IBVE in DCM at 25 °C under a 405 nm LED light (1.1 $mW \cdot cm^{-2}$) with the molar ratio $[IBVE]_0:[CTA]_0:[TPO]_0:[DPI]_0$ = 100:1:0.05:0.05, V_{IBVE}=0.5 mL, V_{DCM}=0.5 mL. (a) $\ln([M]_0/[M])$ versus time, (b) molecular weight (M_n) and molecular weight distribution ($Đ$) versus monomer conversion.

https://doi.org/10.1007/s10118-026-3845-9

Table 2 Polymerization of various monomers in DCM with molar ratio $[Monomer]_0:[CTA]_0:[TPO]_0:[DPI]_0$ = 100:1:0.05:0.05 at 25 °C under a 405 nm LED light (1.1 mW·cm^{-2}), $V_{Monomer}$=0.5 mL, V_{DCM}=0.5 mL.



Entry	Monomer	Time (min)	Conv. (%)	$M_{n,th}$ [a]	$M_{n,SEC}$ [b]	$Đ$
1	EVE	1	94	7000	5600	1.30
2	PVE	2	76	6800	7800	1.17
3	BVE	1	98	10000	8200	1.28
4	DHF	0.5	>99	7200	3600	1.56
5	CHVE	0.5	>99	12700	8500	1.38

[a] Calculated based on conversion ($M_{n,th}$ = $[monomer]_0/[CTA]_0 \times M_{Monomer}$ ×conversion + M_{CTA}); [b] Determined by tetrahydrofuran (THF) SEC using polystyrene (PS) calibration (note: these values are relative molecular weights for poly(vinyl ether)s).

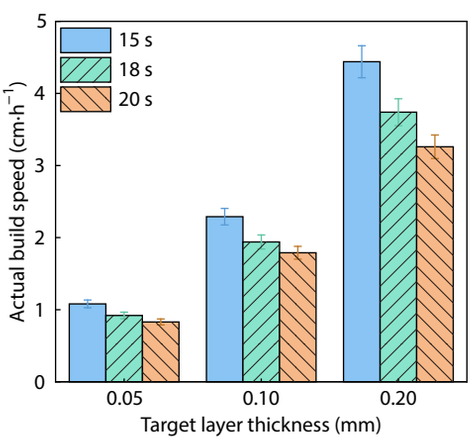


Fig. 3 Printing speed of different printing thickness/time per layer with a molar ratio of $[DDE]_0:[DHF]_0:[CTA]_0:[TPO]_0:[DPI]_0$ = 50:50:1:0.1:0.1.

RAFT-based DLP 3D printing for rapid fabrication of transparent living polymer networks with complex architectures. Notably, the printed objects gradually developed a pale yellow color after several days, which is likely attributable to the decomposition of residual photoinitiators.

The mechanical properties of the printed materials were evaluated by using a series of resin formulations. As shown in Fig. 5(a) and Table S3 (in ESI), increasing the DHF content simultaneously enhanced both the Young's modulus (from 254.80 MPa to 364.81 MPa) and elongation at break (from 15.94% to 36.55%). This behavior was attributed to the formation of high-molecular-weight poly(DHF), which served as a tough thermoplastic component within the crosslinked network.[25] In addition, increasing the CTA concentration resulted in a gradual decrease in the tensile strength, accompanied by an increase in Young's modulus (from 412.57 MPa to 110.34 MPa) accompanied by an increase in elongation at break (from 18.68% to 34.76%) (Fig. 5b). This trend suggests

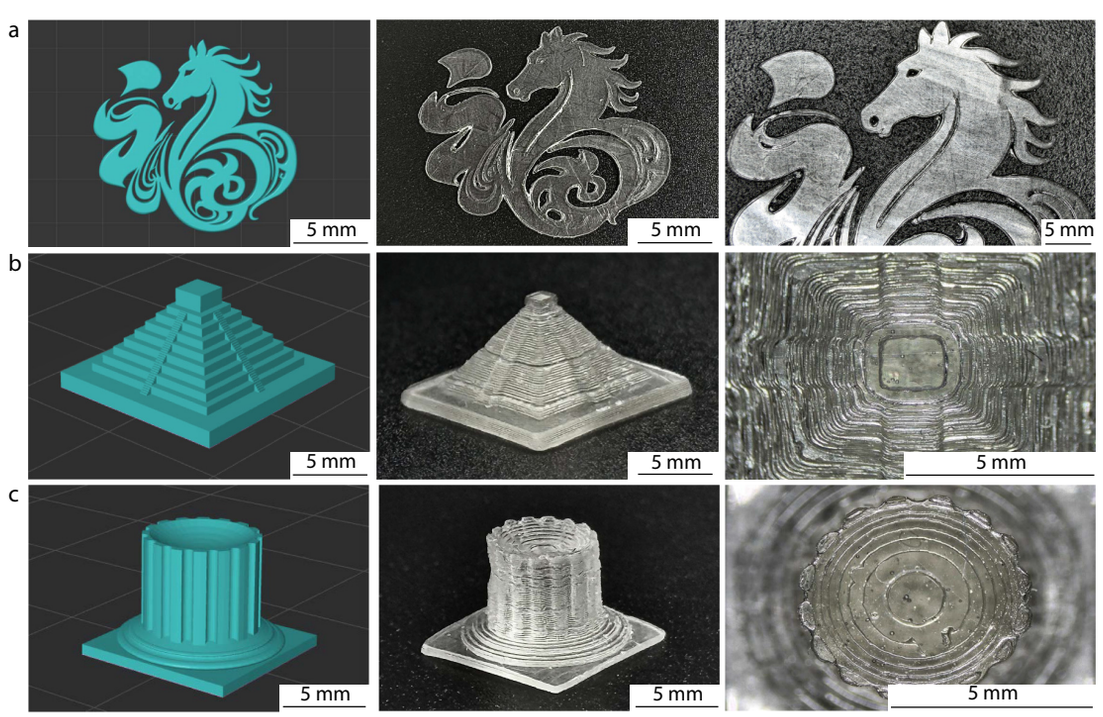


Fig. 4 The printed 3D objects and enlarged digital image of different models ($[DDE]_0:[DHF]_0:[CTA]_0:[DPI]_0:[TPO]_0$ = 50:50:5:0.1:0.1): (a) the character "fortune", (b) Mayan pyramid, (c) Roman column.

https://doi.org/10.1007/s10118-026-3845-9

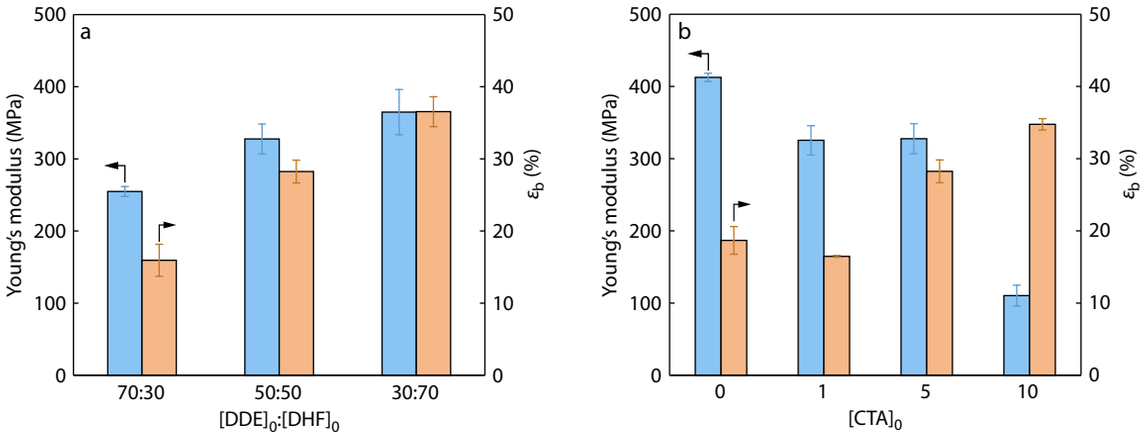


Fig. 5 Tensile testing results of the printed samples obtained by printing resins consisting: (a) $[DDE]_0$:$[DHF]_0$:$[CTA]_0$:$[TPO]_0$:$[DPI]_0$ = *x*:*x*:5:0.1:0.1; (b) $[DDE]_0$:$[DHF]_0$:$[CTA]_0$:$[TPO]_0$:$[DPI]_0$ = 50:50:*x*:0.1:0.1.

that higher CTA concentrations improve network homogeneity by suppressing localized over-crosslinking and reducing structural defects, thereby enhancing the ductility during deformation. Overall, the mechanical properties can be readily tailored by adjusting the DHF content and CTA concentration without compromising printability. These findings further highlight the potential of the present system for the fabrication of transparent, mechanically tunable, living 3D-printed materials.

CONCLUSIONS

In summary, we developed a rapid DLP 3D printing platform based on photoinduced RPC-RAFT polymerization employing a colorless "green" chain transfer agent. The combination of DPI and TPO enables efficient cationic RAFT polymerization under 405 nm irradiation, achieving high monomer conversions within minutes while maintaining good control over molecular weight and molecular weight distribution. The system exhibits broad applicability to vinyl ether monomers and can be readily translated into photocurable resins for DLP printing. Consequently, colorless and highly transparent living polymer networks with excellent printing fidelity were fabricated at practical printing speeds. Moreover, the mechanical properties of the printed materials can be conveniently tailored by varying the resin composition, while preserving excellent printability. Compared with conventional cationic RAFT systems, the present approach eliminates the undesirable coloration associated with visible-light-absorbing CTAs, while retaining the advantages of living polymerization. This study broadens the scope of controlled polymerization-enabled additive manufacturing and provides a versatile platform for fabricating transparent, mechanically tunable, and functional 3D-printed materials for applications in optics, microfluidics, and advanced manufacturing.

Conflict of Interests

The authors declare no interest conflict.

Electronic Supplementary Information

Electronic supplementary information (ESI) is available free of charge in the online version of this article at http://doi.org/10.1007/s10118-026-3845-9.

Data Availability Statement

The data supporting the findings of this study are available from the corresponding authors upon reasonable request.

ACKNOWLEDGMENTS

This work was financially supported by the National Natural Science Foundation of China (Nos. 22371199 and 22571219), Suzhou Cutting-edge Technology Research Project (No. SYG202350), Priority Academic Program Development (PAPD) of Jiangsu Higher Education Institutions, Program of Innovative Research Team of Soochow University, and Undergraduate Training Program for Innovation and Entrepreneurship, Soochow University (No. 202510285051).

REFERENCES

1 Gauci, S. C.; Vranic, A.; Blasco, E.; Brase, S.; Wegener, M.; Barner-Kowollik, C. Photochemically activated 3D printing inks: current status, challenges, and opportunities. *Adv. Mater.* **2024**, *36*, 2306468.
2 Wang, Y.; Cui, H.; Esworthy, T.; Mei, D.; Wang, Y.; Zhang, L. G. Emerging 4D printing strategies for next-generation tissue regeneration and medical devices. *Adv. Mater.* **2022**, *34*, 2109198.
3 Bao, Y.; Paunović, N.; Leroux, J. C. Challenges and opportunities in 3D printing of biodegradable medical devices by emerging photopolymerization techniques. *Adv. Funct. Mater.* **2022**, *32*, 2109864.
4 Narupai, B.; Nelson, A. 100th Anniversary of macromolecular science viewpoint: macromolecular materials for additive manufacturing. *ACS Macro Lett.* **2020**, *9*, 627−638.
5 Bagheri, A.; Jin, J. Photopolymerization in 3D printing. *ACS Appl. Polym. Mater.* **2019**, *1*, 593−611.
6 Corrigan, N.; Jung, K.; Moad, G.; Hawker, C. J.; Matyjaszewski, K.; Boyer, C. Reversible-deactivation radical polymerization (controlled/living radical polymerization): from discovery to materials design and applications. *Prog. Polym. Sci.* **2020**, *111*,

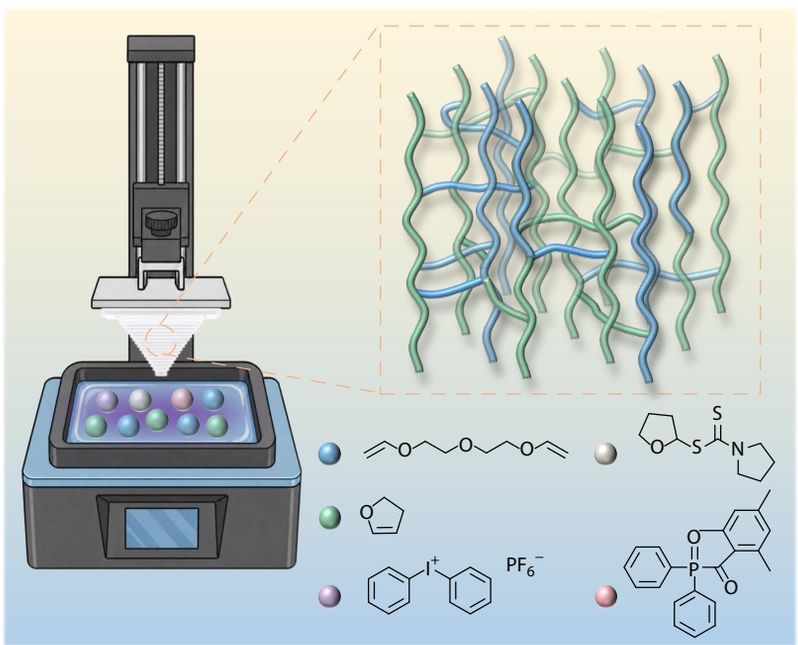
Graphical Abstract

Photoinduced Cationic Reversible Addition–Fragmentation Chain Transfer 3D Printing Using 'Green' Chain Transfer Agent

Ying Zhu, Wen-Hui Li, Shu-Han Ling, Fukuda Shinichiroh, Zhi-Hua He, Jia-Jia Li, and Jian Zhu

Soochow Universitya; Taiyo Ink Suzhou Co. Ltd.

A photoinduced radical-promoted cationic reversible addition–fragmentation chain transfer (RPC-RAFT) polymerization system employing a colorless chain transfer agent is developed for digital light processing (DLP) 3D printing.



Chinese J. Polym. Sci. 2026 *https://doi.org/10.1007/s10118-026-3845-9*

101311.

7 Zhou, Y. N.; Li, J. J.; Wang, T. T.; Wu, Y. Y.; Luo, Z. H. Precision polymer synthesis by controlled radical polymerization: fusing the progress from polymer chemistry and reaction engineering. *Prog. Polym. Sci.* **2022**, *130*, 101555.

8 Parkatzidis, K.; Wang, H. S.; Truong, N. P.; Anastasaki, A. Recent developments and future challenges in controlled radical polymerization: a 2020 update. *Chem* **2020**, *6*, 1575–1588.

9 Zhang, Z.; Corrigan, N.; Boyer, C. A versatile 3D and 4D printing system through photocontrolled RAFT polymerization. *Angew. Chem. Int. Ed.* **2019**, *58*, 17954–17963.

10 Lee, K.; Corrigan, N.; Boyer, C. Rapid high-resolution 3D printing and surface functionalization via type I photoinitiated RAFT polymerization. *Angew. Chem. Int. Ed.* **2021**, *60*, 8839–8850.

11 Bagheri, A.; Engel, K. E.; Bainbridge, C. W. A.; Xu, J.; Boyer, C.; Jin, J. 3D printing of polymeric materials based on photo-RAFT polymerization. *Polym. Chem.* **2020**, *11*, 641–647.

12 Bagheri, A.; Bainbbridge C. W. A.; Engel K. E.; Qiao G. G.; Xu J.; Boyer C.; Jin J. Oxygen tolerant PET-RAFT facilitated 3D printing of polymeric materials under visible LEDs. *ACS Appl. Polym. Mater.* **2020**, *2*, 782–790.

13 Belqat, M.; Wu, X.; Morris, J.; Mougin, K.; Petithory, T.; Pieuchot, L.; Guillaneuf, Y.; Gigmes, D.; Clément, J. L.; Spangenberg, A. Customizable and reconfigurable surface properties of printed micro-objects by 3D direct laser writing via nitroxide mediated photopolymerization. *Adv. Funct. Mater.* **2023**, *33*, 2211971.

14 Jia, Y.; Spiegel, C. A.; Welle, A.; Heißler, S.; Sedghamiz, E.; Liu, M.; Wenzel, W.; Hackner, M.; Spatz, J. P.; Tsotsalas, M.; Blasco, E. Covalent adaptable microstructures via combining two-photon laser printing and alkoxyamine chemistry: toward living 3D microstructures. *Adv. Funct. Mater.* **2022**, *33*, 2207826.

15 Qiao, L.; Zhou, M.; Shi, G.; Cui, Z.; Zhang, X.; Fu, P.; Liu, M.; Qiao, X.; He, Y.; Pang, X. Ultrafast visible-light-induced ATRP in aqueous media with carbon quantum dots as the catalyst and its application for 3D printing. *J. Am. Chem. Soc.* **2022**, *144*, 9817–9826.

16 Bobrin, V. A.; Zhang, J.; Corrigan, N.; Boyer, C. The emergence of reversible-deactivation radical polymerization in 3D printing. *Adv. Mater. Technol.* **2023**, *8*, 2201054.

17 Bagheri, A. Application of RAFT in 3D printing: where are the future opportunities *Macromolecules* **2023**, *56*, 1778–1797.

18 Uchiyama, M.; Satoh, K.; Kamigaito, M. Cationic RAFT

polymerization using ppm concentrations of organic acid. *Angew. Chem. Int. Ed.* **2015**, *54*, 1924–1928.
19 Uchiyama, M.; Satoh, K.; Kamigaito, M. Cationic RAFT and DT polymerization. *Prog. Polym. Sci.* **2022**, *124*, 101485.
20 Kamigaito, M.; Sawamoto, M. Synergistic advances in living cationic and radical polymerizations. *Macromolecules* **2020**, *53*, 6749–6753.
21 Zhao, B.; Li, J.; Li, G.; Yang, X.; Lu, S.; Pan, X.; Zhu, J. Fast living 3D printing via free radical promoted cationic RAFT polymerization. *Small* **2023**, *19*, 2207637.
22 Zhao, B.; Li, J.; Yang, C.; Pan, X.; Zhang, Z.; Zhu, J. Rapid and high-resolution 3D printing via photoacid generator induced cationic RAFT polymerization. *Sci. China Chem.* **2025**, *68*, 2010–2016.
23 Spring, S. W.; Cerione, C. S.; Hsu, J. H.; Shankel, S. L.; Fors, B. P. Scalable, green chain transfer agent for cationic RAFT polymerizations. *Chin. J. Chem.* **2022**, *41*, 399–404.
24 Sifri, R. J.; Kennedy, A. J.; Fors, B. P. Photocontrolled cationic degenerate chain transfer polymerizations via thioacetal initiators. *Polym. Chem.* **2020**, *11*, 6499–6504.
25 Spring, S. W.; Hsu, J. H.; Sifri, R. J.; Yang, S. M.; Cerione, C. S.; Lambert, T. H.; Ellison, C. J.; Fors, B. P. Poly(2,3-dihydrofuran): a strong, biorenewable, and degradable thermoplastic synthesized via room temperature cationic polymerization. *J. Am. Chem. Soc.* **2022**, *144*, 15727–15734.

https://doi.org/10.1007/s10118-026-3845-9